Journal of Energy Technologies and Policy
ISSN 2224-3232 (Paper) ISSN 2225-0573 (Online)
Vol.11, No.1, 2021

Investigation of Impact of Contingencies on Power Plant and Transmission Lines

UGWU K .I
Department of Electrical Electronic Engineering,
Enugu State University of Science & technology (ESUT), Enugu, Nigeria

Abstract
Contingency analysis are widely applied to predict the effect of outages in power systems, like tripping of equipment in power plants and transmission lines. Using off line analysis to predict the effect of individual contingency is a tedious task on power system containing large number of components. Practically, only selected contingencies will lead to severe conditions in power system, like violation of voltage and active power flow limits. Simultaneously, the value of active power flow before and after severe transmission and power plant contingencies was analysed using Genetic Eigenvalue Analysis Technique. This was achieved by simulating the Simulink of Nigerian 330KV 48 bus power system using m-file programme in MATLAB environment.The result of the simulation for the power flow solution for transmission line outage contingencies shows that the voltage trajectory at bus 11 stood at 0.3934 p.u, at bus 15 is0.4986 p.u, and bus of 23 is 0.4647 p.u while for the contingencies on power plant, there voltage trajectories stood at 0.2342 p.u for bus 11, 0.3987 p.u for bus 23. The result shows that the impact on power plant is higher than that of transmission line by 40%, 20%, 14%for sampled buses 11, 15, and 23 respectively.
Keywords: Power Stability- Genetic Eigenvalue, Load flow
DOI: 10.7176/JETP/11-1-04
Publication date: January 31st 2021

1.1INTRODUCTION:

This paper presents an efficient and realistic contingency analysis method of Nigerian 330KV power system using Genetic Eigenvalue Technique.

The purpose and usefulness of small signal stability investigation is to understand the characteristics of system behavior with minimal error while significantly decreasing both the complexity and scale of computation involved. With the size and complexity of power systems ever increasing, the computational effort involved can easily surpass feasible limits even when utilizing computers and other speed processing equipment. As a result, simplified techniques can be used to yield rather precise and useful characteristics of a system that in turn, indicate system response and behavior, all while greatly reducing the effort involved. The term “small signal” reflects the minor disturbances used to evaluate the simplified system model. Small disturbances within a system are common and refer to disturbances that allow representation of the nonlinear system as a linearized model Hoang[7]. These disturbances can include load changes, and various oscillations and resonance within a power system. So what is the general idea behind small signal stability? As mentioned earlier, small signal stability takes a power system relation involving complex nonlinearities and analyzes a stable system around an equilibrium point as it experiences small perturbations. This is done by linearizing the system around a point or utilizing other techniques that eliminate complex dynamics. This effectively takes a nonlinear system and transforms it into a linear system where many assumptions and simplifications can be made. It is important to note that the linear approximation is only made at a certain point and changes at each different point in time. Conversely, transient stability analysis refers to the analysis of power systems accounting for the nonlinear dynamics of the modeled system. Larger disturbances justify analysis of the system’s response at different operating points as the system characteristics change. Transient stability analysis differs in the type and degree of disturbance but can often decompose into a state similar to small signal instability. Concerning transient instability, synchronization issues can result from first swing issues or long term end state instability can result from growing oscillations.

2.1 REVIEW OF OTHER RESEARCH WORK

Taguchi method has been employed to solve economic dispatch problems [5].Power system stabilizer (PSS) PSS provide better damping over a wide range of operating conditions. Finally, it can be concluded that the Taguchi principle can be effectively employed to achieve an intrinsic robustness in the PSS parameters against variations in operating conditions.

The model done by[6], was tested on the 16-machine in 68- bus New England-New York interconnected system, and its effectiveness was established during the Eigenvalue analysis and nonlinear simulation results. In addition, the results demonstrated that the minimum damping ratio can be increased, and the number of PSSs can be reduced by adding UPFC-based stabilizer to the system.

The work of[7],on optimization problem was also formulated to determine PSS placement. The objective was

to minimize the PSS control gains with constraints to move the unstable eig10nvalues to the stable region while not changing the stable eigenvalues. This approach assumed that PSSs were installed at every machine.

During severe disturbance, a PSS may actually cause the generator under its control to lose synchronism in an attempt to control its excitation [8].

GAGenetic Algorithm has been applied successfully to various power system problems and the recent approach is to integrate the use of GA and fuzzy logic systems in order to design power system stabilizer [3].The coordination between genetic based fuzzy logic power system stabilizer (GFLPSS) and CPSS provide good damping characteristics during small disturbance and large disturbances for local as well as inter area modes of oscillations

The closed-loop performance of the system model was evaluated for an input disturbance in the mechanical torque. The results show that the optimal output controller exhibits better performance than the conventional controller. Results also show the robustness and the validity of the output optimal controller. The usage of optimal control is discussed[9].

3.1 RESEARCH METHODOLOGY:

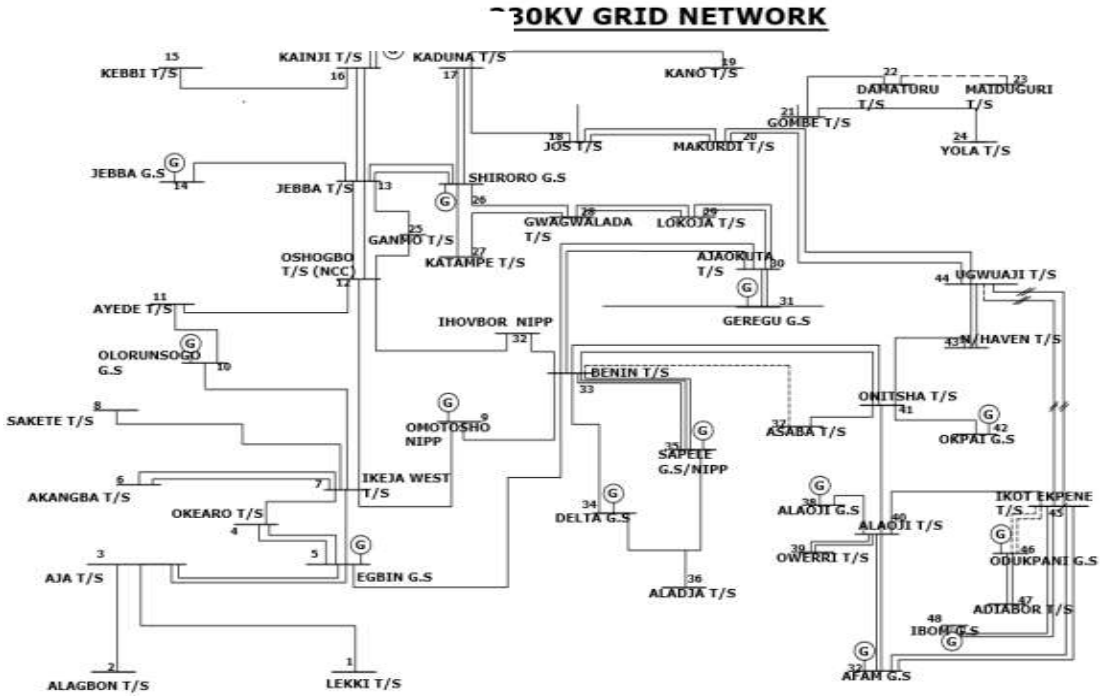

Figure 1: The Nigerian 330kv, 48-Bus Line Diagram

The Nigerian 330KV, 48-bus system was modeled as the case study power system for the simulation test, to validate the stability analysis technique and the proposed power system damping controller. The MATLAB Simulink environment is used for the modeling and development of the case study interconnected power system damping controller and for programming the genetic-eigenvalue stability analyzer. For the testing and evaluation of the solution, different transient disturbances were simulated and injected into the MATLAB model of the case study power grid to investigate the performance of the system. Simulations are carried out to determine the effect on the power system angle stability, voltage stability and frequency stability of the case study of power system.

3.2Development of Simulink Model of the Case Study Power system

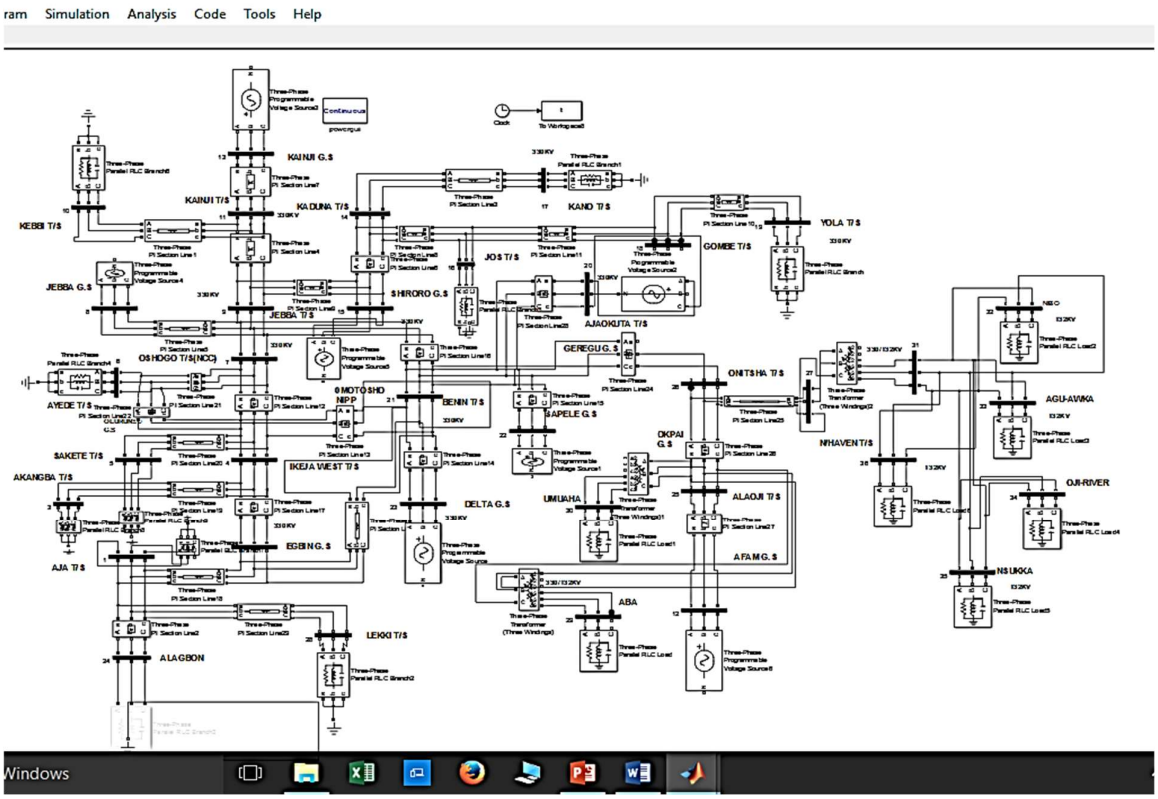

Figure 2:*Simulink Model of the Nigerian 330KV Power System*

The Simulink model of Nigerian 330KV, 48-bus interconnected system was developed for load flow studies, to see the base case voltage profile of the network and for further simulations on the implementation of genetic eigenvalue algorithm

The Nigerian 330KV, 48-bus was modeled using MATLAB Simulink tool box. This shows 48-bus for further simulations on the network as shown on fig 2.System data for the existing 48-bus Nigeria 330kV power networks obtained from Power Transmission Company of Nigeria (TCN) Osogbo, were used as input data which provided the values of series impedances, admittances of the transmission lines, transformer ratings and impedances required for the power/load flow study. These parameters were modeled and simulated in MATLAB/SIMULINK power system analysis using Newton-Raphson power flow algorithm.

3.3 Load/ Power Flow solution for 48-bus network.

Nigerian 330KV 48-bus modeled using MATLAB/SIMULINK Simulation power toolbox.The MATLAB M-file program $Pflow$ was then used to carry out load flow solution of the 48-bus 330KV interconnected power system. The source code of the $Pflow$software. The $Pflow$ load flow software implements the Newton-Raphson load flow algorithm. The load flow was done to obtain the base case voltage profile of the case study power system. From the load flow investigation, it can be seen that 27 buses are below the 5% voltage drop limit. This shows substantial weakness in the power system under investigation. However, this does not give much information regarding the distribution of instabilities in the system. The power system stability is now analyzed under generator outage condition. The MATLAB SIMULINK synchronous generator block was configured to trip the generator within a set time. The block is configured to trip generator 4 within 1.5secs of the simulation. The result of associated eigenvalue analysis is as analyzed below.

3.4 Mathematical Model of Power Flow and Eigenvalue Analysis

Power system matrices are required for the stability analyses of genetic eigenvalue analysis program, hence the mathematical model were derived as shown

$$I = YV = \frac{S*}{V*} \qquad (1)$$

Where

I = Modal current injection matrix
Y = System modal admittance
V = Unknown complex mode voltage vector
S = Apparent power modal injection vector representing specified load and generation of nodes.

Where

$$S = P + JQ \quad (2)$$

The using Newton-Raphson method from (3), the equation for node K (bus K) is written as:

$$I_K \sum_{m=1}^{n} Y_{KM}\, V_m \quad (3)$$

$$P_K + JQ_k = V_K I_K = V_K \sum_{m=1}^{n} Y_{KM}\, V_m \quad (4)$$

Where

M = 1, 2 ……. n
n = number of buses
V_k is the voltage of the K bus
Y_{KM} is the element of the admittance bus equating the real and imaginary parts

$$P_K = K_e\left(V_K\left(\sum_{m=1}^{n} Y^*_{KM} V^*_K\right)\right) \quad (5)$$

$$Q_K = I_M\left(V_K\left(\sum_{m=1}^{n} Y^*_{KM} V^*_K\right)\right) \quad (6)$$

Where

P_K is the real power
Q_K is the reactive power with the following notation:

$$V_K = |V_K|e^{jq_k}, V_M = |V_m|e^{jq_m}, Y_{KM^2}|Y_{KM}|e^{jt} \quad (7)$$

Where

$|V_K|$ is the magnitude of the voltage
δ_k is the angle of the voltage
δ_{km} is the load angle

Substituting for $V_k, V_m,$ and Y_{km} in equation (8)

$$P_K + JQ_K = |V_K|e^{jd_k}\sum_{m=1}^{n} |V_k||Y_{KM}|e^{jq_{km}} \quad (9)$$

$$P_K + JQ_K = |V_K|\sum_{m=1}^{n} |V_k||Y_{KM}|e^{j(\delta_k - \delta_m = \delta_{km})} \quad (10)$$

Or

$$P_K + JQ_K = |V_K|\sum_{m=1}^{n} |V_k||Y_{KM}| < (\delta_k - \delta_k - \delta_{km}) \quad (11)$$

Or

$$+JQ_k = |V_K|\sum_{m=1}^{n} |V_k||Y_{KM}|(\cos\delta_k - \delta_m - Q_{km}) + J\sin(\delta_k - \delta_m - Q_{km}) \quad (12)$$

Separating the real and imaginary parts of above equations to get real and reactive power

$$P_K = |V_K| \sum_{m=1}^{n} |V_k||Y_{KM}| \cos(\delta_k - \delta_m - Q_{km}) \quad (13)$$

$$Q_K = |V_K| \sum_{m=1}^{n} |V_k||Y_{KM}| \sin(\delta_k - \delta_m - Q_{km}) \quad (14)$$

The mismatch power at bus K is given by:

$$\Delta P_K = P_K^{sch} - P_K \quad (15)$$

$$\Delta Q_K = Q_K^{sch} - Q_K \quad (16)$$

The P_K and Q_K are calculated from equations (3.13) and (3.14)

The Newton – Raphson method solves the partitioned matrix equation:

$$\begin{bmatrix} \Delta P \\ \Delta Q \end{bmatrix} = J \begin{bmatrix} \Delta Q \\ \Delta V \end{bmatrix} \quad (17)$$

Where

ΔP and ΔQ = mismatch active and reactive power vectors

ΔV and ΔQ = unknown voltage magnitude and angle correction vectors

J = Jacobean matrix of partial derivative terms

The eigenvalues associated with a mode of voltage and reactive power variation can provide a relative measure of proximity to voltage instability. Then, the participation factor can be used to find out the weak nodes or buses in the system.

Equation (15) can be written as:

$$\begin{bmatrix} \Delta P \\ \Delta Q \end{bmatrix} = \begin{bmatrix} J_{11} & J_{12} \\ J_{21} & J_{22} \end{bmatrix} \begin{bmatrix} \Delta Q \\ \Delta V \end{bmatrix} \quad (18)$$

By letting $\Delta P = O$ in Equation (3.18)

$$\Delta P = O = J_{11}\Delta\theta + J_{12}\Delta V \quad (19)$$

Where

$$\Delta\theta = -J_{11}^{-1} J_{12}\Delta V \quad (20)$$

$$\Delta\theta = -J_{21} \Delta\theta + J_{22}\Delta V \quad (21)$$

Subtracting equation (17) in equation (21)

$$\Delta\theta = -J_R \Delta V \quad (22)$$

Where

$$J_R = \left[J_{22} - J_{21}J_{11}^{-1}J_{12}\right]$$ J_R is the reduced jacobian matrix of the system

Equation (13) can be written as

$$\Delta V = J_R^{-1}\Delta Q \quad (23)$$

The matrix J_R represents the linearized relationship between the incremental changes in bus voltage (ΔV) and bus reactive power injection (ΔQ). It is well known that the system voltage is affected by both real and reactive power variations. In order to focus the study of the reactive demand and supply problem of the system as well as minimize computations effort by reducing dimension of the computation effort by reducing dimensions of the Jacobean Matrix J the real power $(\Delta P = O)$ and angle part from the system his equation (3.13) are eliminated..

The eigenvalues and Eigen-vectors of the reduced order Jacobean matrix (J_R) are used for the power system stability characterized analysis. Instability can be detected by identifying modes of the eigenvalues matrix (J_R). The magnitude of the eigenvalues provides a relative measure of proximity to instability. The eigenvectors on the other hand present information related to the mechanism of loss of voltage stability.

Modal analysis of (J_R) results in the following

$$(J_R) = \tau\phi\xi_{eigl} \tag{24}$$

Notation used in the flow chart:

$A = (J_R)$ is the system matrix, based on the model of the power system

$H$is matrix having orthonormal columns

$V$is matrix having orthonormal columns (can also be an invariant sup space of matrix A)

x, f are the Ritz vectors

$\lambda$is the eigenvalues

σ is a shift

$I$is the identity matrix

ξ_{eigl} = left eigenvector matrix of (J_R)

X = diagonal eigenvalue matrix of (J_R)

Equation (22) can be written as:

$$J_R{}^{-1} = \phi\xi_{eigl} \tag{25}$$

The appropriate definition and determination as to which modes or buses participates in the selected mode become very important. The participation factor is computed to identify the weakest nodes or lead buses that are making significant contribution to the selected modes.

The participation factor is given by

$$X_i = \frac{\sum \phi_i \xi_{ei\lambda l}}{\lambda_i} \Delta Q \tag{26}$$

Whereλ_i is the i^{th} eigenvalue, ϕ_i is the column right eigenvector and is the i^{th} column right eigenvector and $\xi_{ei\lambda l}$ is the i^{th} row left eigenvector of matrix (J_R)

Each eigenvalue and corresponding right and left eigenvectors ϕ_i and $\xi_{ei\lambda l}$, defines the i^{th} modes of the system.

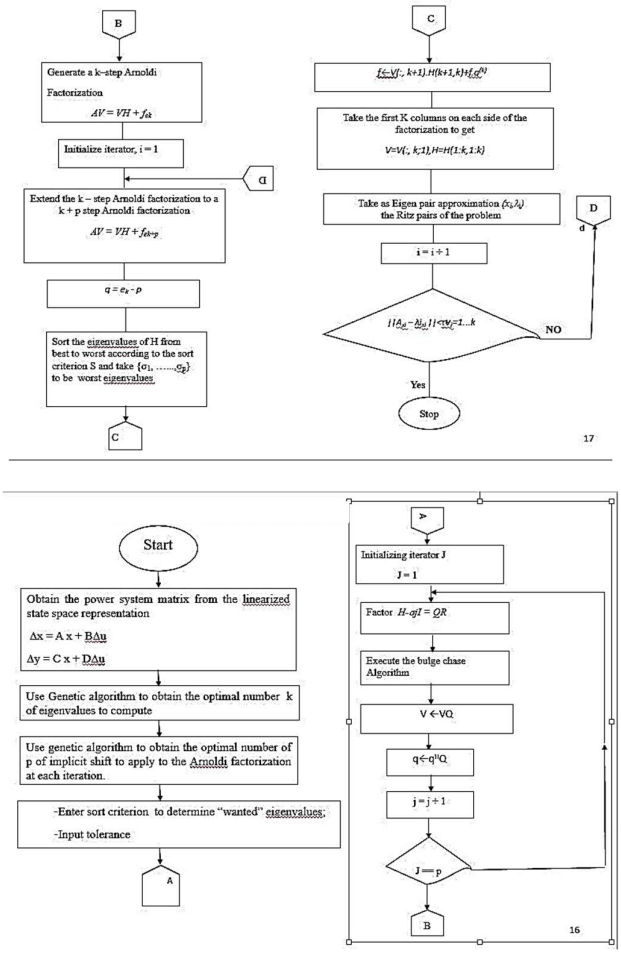

Fig 3: Flow Chart for Genetic Eigenvalue programming

The flow chart for the implementation of the Genetic eigenvalue algorithm programming was developed as shown in fig 3 contains an arranged parameters for simulation and generation of eigenvalues, and computation of participation factors and damping ratios of the Nigerian 330KV 48-Bus network from the network Simulink of figure 3. The genetic eigenvalue stability analysis program, the eigenvalues of the network are extracted, participation factors and damping ratios of the generators were equally computed by the program.

4. RESULTS

The base data for this paper are system parameters of Nigerian 330KV 48-bus system from Transmission Company of Nigeria. There are 14 synchronous generators in the system. The base voltage is 330KVA and 100MVA. The generator, line and bus parameters used for simulation and computations are listed in table 1.

Table 1: The Generator Parameters

S/No	Generator Station	Generation	Rated Voltage	Voltage P.U
1	Kainji	292Mw	332KV	1.0060
2	Jebba	404Mw	312KV	0.9455
3	Shiroro	450Mw	320KV	0.9697
4	Egbini	611Mw	335KV	1.0151
5	Sapele	68Mw	332KV	1.0060
6	Delta	470Mw	318KV	0.9636
7	Geregu	144Mw	319KV	0.9677
8	Omotosho	187.5Mw	305KV	0.9242
9	Olominsogo gas	163.6Mw	300KV	0.9090
10	Geregu NIPP	150Mw	331KV	1.0030
11	Sapele NIPP	113.1Mw	320KV	0.9692
12	Olorunsogo NIPP	130.9Mw	316KV	09576

S/No	Generator Station	Generation	Rated Voltage	Voltage P.U
13	Omotosho NIPP	228Mw	347KV	1.05151
14	Okapia	363Mw	331KV	1.0030

Bus Parameter

System Details

MVA Base = 100MVA

System frequency = 50Hz

Bus Nominal Voltage = 330KV

Bus Maximum Voltage = 330.5kv

Type:

1 = Load Bus

2 = Generator Bus (pv)

3 = System Wiring Bus

Table 2: Bus Parameters

Bus No	Type	Max-Vm-Pu	Min-Vm-Pu	Area	Zone	In-Service	Vn-KV
1	2	1.05	0.95	1	1	True	330KV
2	2	1.05	0.95	1	1	True	330KV
3	2	1.05	0.95	1	1	True	330KV
4	2	1.05	0.95	1	1	True	330KV
5	2	1.05	0.95	1	1	True	330KV
6	2	1.05	0.95	1	1	True	330KV
7	2	1.05	0.95	1	1	True	330KV
8	2	1.05	0.95	1	1	True	330KV
9	2	1.05	0.95	1	1	True	330KV
10	2	1.05	0.95	1	1	True	330KV
11	2	1.05	0.95	1	1	True	330KV
12	2	1.05	0.95	1	1	True	330KV
13	2	1.05	0.95	1	1	True	330KV
14	2	1.05	0.95	1	1	True	330KV
15	2	1.05	0.95	1	1	True	330KV
16	2	1.05	0.95	1	1	True	330KV
17	2	1.05	0.95	1	1	True	330KV
18	2	1.05	0.95	1	1	True	330KV
19	2	1.05	0.95	1	1	True	330KV
20	2	1.05	0.95	1	1	True	330KV
21	2	1.05	0.95	1	1	True	330KV
22	2	1.05	0.95	1	1	True	330KV
23	2	1.05	0.95	1	1	True	330KV
24	2	1.05	0.95	1	1	True	330KV
25	2	1.05	0.95	1	1	True	330KV
26	2	1.05	0.95	1	1	True	330KV
27	2	1.05	0.95	1	1	True	330KV
28	2	1.05	0.95	1	1	True	330KV
29	2	1.05	0.95	1	1	True	330KV
30	2	1.05	0.95	1	1	True	330KV
31	2	1.05	0.95	1	1	True	330KV
32	2	1.05	0.95	1	1	True	330KV
33	2	1.05	0.95	1	1	True	330KV
34	2	1.05	0.95	1	1	True	330KV
35	2	1.05	0.95	1	1	True	330KV
36	2	1.05	0.95	1	1	True	330KV
37	2	1.05	0.95	1	1	True	330KV
38	2	1.05	0.95	1	1	True	330KV
39	2	1.05	0.95	1	1	True	330KV
40	2	1.05	0.95	1	1	True	330KV
41	2	1.05	0.95	1	1	True	330KV
42	2	1.05	0.95	1	1	True	330KV

Bus No	Type	Max-Vm-Pu	Min-Vm-Pu	Area	Zone	In-Service	Vn-KV
43	2	1.05	0.95	1	1	True	330KV
44	2	1.05	0.95	1	1	True	330KV
45	2	1.05	0.95	1	1	True	330KV
46	2	1.05	0.95	1	1	True	330KV
47	2	1.05	0.95	1	1	True	330KV
48	2	1.05	0.95	1	1	True	330 KV

Table 3: Load Flow Result for the Plot of the Profile of the Base Case Power System

BUS	Voltage(p.u)	Angle(rad)	P gen(p.u)	Q gen(p.u)	P load(p.u)
1	0.9604	-0.03153	4.86E-14	1.4E-12	1.89
2	0.9668	-0.02274	2.4	1.251088	0
3	0.9026	-0.01048	1.15E-13	4.33E-13	4.5
4	0.9702	-0.0254	1.55E-15	-9.4E-15	1.95
5	0.8436	0.087284	3.213	0.004826	0
6	0.7858	-0.00543	-1.1E-13	-5.6E-13	9.18
7	0.9754	0.085714	0.8	0.583475	0
8	0.9118	-0.03631	4.09E-14	9.21E-13	1.545
9	0.9546	-0.08476	2.16	9.594193	1.545
10	0.7598	-0.10347	-1E-14	-1.7E-13	0
11	0.7003	-0.0065	8.08E-14	-1.2E-13	2.424
12	0.9176	0.08684	1.928	0.753387	0
13	0.9731	0.085158	2.71E-13	1.98E-13	2.292
14	0.8760	-0.07592	1.2	-1.84677	0
15	0.9055	0.085664	-7.3E-14	-6.3E-14	0
16	0.7962	-0.13836	-1.3E-13	-1E-13	1.146
17	0.8338	-0.03392	-3E-13	-2.2E-13	1.53
18	0.9569	-0.13756	-3.2E-14	-2.4E-14	0
19	0.9506	-0.03113	1.76	5.189297	1.89
20	0.7517	-0.07522	2.35E-13	9.63E-14	0
21	0.7540	0.085614	-2.9E-13	1.91E-13	2.292
22	0.9535	-0.00585	-9.4E-14	1.06E-12	2.7
23	0.7257	-0.02394	-4.5E-13	-4.6E-14	0
24	0.9691	-0.02655	-4.6E-14	-3.2E-13	1.146
25	0.8899	-0.00946	-1.3E-13	-6.3E-13	3.6
26	0.9436	-0.02736	1.125	0.236856	0
27	0.9621	0.083392	-2.2E-13	-1.3E-13	0
28	0.8587	-0.06639	9.88E-16	2.81E-14	0
29	0.7720	-0.10593	7.99E-15	7.53E-14	1.275
30	0.9754	-0.0242	-2.4E-14	-1.7E-13	1.95
31	0.7431	-0.02572	-1E-14	-1.7E-13	0.73725
32	0.7991	-0.02977	-2.7E-15	-3.1E-14	1.617
33	0.9032	-0.11249	7.24E-15	-2.9E-14	0
34	0.8465	-0.02361	7.82E-13	5.08E-13	1.2471
35	0.9529	-0.13943	-4.3E-14	-3E-14	0.615
36	0.9801	-0.02648	2.4	0.104634	0
37	0.9529	0	46.0197	9.032308	0
38	0.9853	-0.14123	-1.9E-14	2.61E-14	0.573
39	0.9639	-0.03703	-5.1E-15	-1.2E-14	1.545
40	0.9766	-0.02195	2.4	-0.33846	0
41	0.9303	-0.13818	4.2E-14	1.86E-13	1.548
42	0.9673	-0.04831	-6E-15	1.44E-14	1.8609
43	0.9147	-0.14204	1.104	1.672078	0
44	0.9598	-0.03259	1.42E-14	8.36E-14	0.91725
45	0.8477	-0.01242	4.56	0.542995	0.6225
46	0.9587	-0.01106	-6.5E-14	3.14E-13	6.29
47	0.8205	-0.53696	3.29E-13	3.79E-14	1.65
48	0.9014	-0.02617	4.416	0.667066	0.765

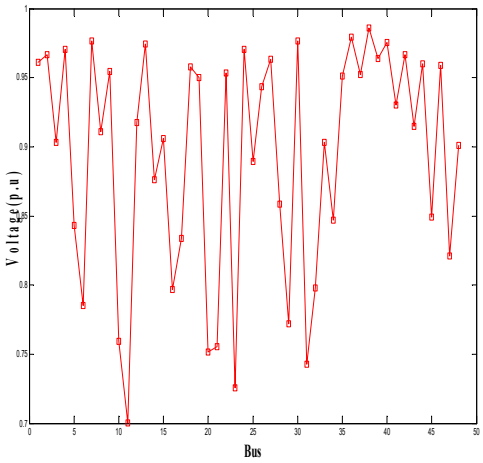

Figure. 4: Voltage Profile of the Base Case of Nigerian 330KV Power System

From the load flow result, it can be seen that 27 buses are below the 5% voltage drop limit. This shows substantial weakness in the power system under investigation which might lead to instability.. However, this does not give much information regarding the distribution of instabilities in the system. Hence further simulations were carried out using the hybrid of Genetic and Arnoldi Eigenvalue analysis technique to find the eigenvalues, the damping ratios and the participation factors in the power system for proper placement of Power System Stabilizers Result of Pflw solution on outage of transmission line without stabilizer.

4.2 Simulation and Analysis of Voltage Stability

Simulations were carried out to determine the base voltage stability levels at the buses of the case study power system, and the ability of the system to operate stably and also to remain stable following the injection of simulated contingencies. The Eigenvalue analysis program was applied to the case study power system modeled in MATLAB simulink as shown in figure 2, The MATLAB m-file code of the eigenvalue program interfaces with the MATLAB/SIMULINK model of the case study power system via the MATLAB program Workspace.

The bus eigenvalues, bus participation factor, and bus damping ratios were computed for the case study power system base operational state (i.e. For the power system steady state – without contingency or disturbances) is listed in table 4.

Table 4: Load Flow Result for the Plot of the Profile of the Base Case Power System

#	Bus #	Eigen value(λ)	Damping ratio(G) 1× 10^{-1}	Participation factor (%)
1	8	- 5.5957±j10.3330	0.04762	0.0102
2	9	2.325±j8.0321	0.02781	2.0018
3	10	-5.6837±j10.3601	0.04810	0.2146
4	11	-2.4892±j10.8650	0.02233	10.1575
5	12	-0.4087±j0.8293	0.4421	0.0625
6	13	-0.8922±j3.013	0.2842	3.1174
7	14	-5.3063±j10.3295	0.4569	0.0625
8	15	-5.1617±j11.2755	0.4162	12.4678
9	16	-0.4759±j0.5616	0.6465	0.0933
10	17	-04164±j0.6618	0.5325	0.0536
11	18	-2.0922±j7.914	0.2562	2.0341
12	19	-1.1731±j4.1051	0.2751	4.3210
13	20	-0.8042±j2.9632	0.2623	0.7326
14	21	-1.1843±j3.845	0.2942	3.0072
15	22	-1.1012±j3.1752	0.3283	0.4136
16	23	0.9499±j3.5917	0.2552	2.0018
17	24	-4.0428±j5.80451	0.5716	1.4172
18	25	-5.5160±j5.22030	0.7108	8.3066
19	26	-3.7688±j6.0058	0.5315	3.4172
20	27	3.2505±j82795	0.36543	0.9847
21	28	-2.8394±j7.8648	0.3396	2.6731
22	29	-2.6431±j8.0318	0.3126	0.9874
23	30	-2.9202±j7.7275	0.3536	0.0378

The Eigenvalue (λ) give information about the proximity of the system to instability. The participation factor measure the participation of a state variable in a certain mode of oscillation [12]. The bus participation factor

shows the weak zones of the system (Montano et al, 2006). The branches and the generator participation factors shows transmission lines with the most reactive consumption and the generator that mainly supply reactive power back to the system[1]. The damping ratios (ς) is an indication of ability of the system to return to stable state in the event of disturbance.

4.3 Contingencies without the Power System Stabilizers Installed/Outage of One Transmission Line

A transmission line outage increases line impedance and weakens inter connection. Due to the increase in line reactance, extra reactive power is needed in other to maintain the voltage at the load buses. Here, the transmission outage simulation is performed by opening the line between bus 31 and bus 29 and reclosing it after five cycles. The circuit breaker in the SIMULINK library are configurable .The circuit breaker between bus31 and 29 was configured to open in 1 second and reclose after five cycle.

The Genetic Eigenvalue computation program was called during the simulation to compute the system eigenvalue, damping ratio and participation factor at the system buses. The power flow program was activated to carry out power flow solution of the current state of the power system. From result of the eigenvalue analysis almost all the real part of the complex eigenvalue listed in table 4 lie on the right half of the S-plain. That is the real parts of the complex eigenvalue are almost all positive. This is an indication that the system is unstable. The damping ratios of the eigenvalue are very small. The negative value of most of the damping ratios is a further indication of the instability of the system. Bus 11 shows the most negative (smallest) damping ratio (being the weakest bus even at steady state) the damping ratio of most of the buses in the power system during the disturbance are below the 5% minimum and the 0.2 damping threshold .The listing in table 5 confirms the information from the eigenvalue analysis.

The values in table 6 show that there is serious voltage degradation at the buses of the power system. The voltages in most of the buses are degraded. These result indicate that the exciters on the generators alone cannot stabilize the oscillation in the power system. The voltage magnitudes in table 6 do not give complete information of variation of voltage at the buses. The eigenvalues and the damping ratios indicates that the power system is unstable. This means that voltage at nodes of the power system are oscillating.

The trajectory of the voltage at the buses 11, 15 and 23, as a result of the transmission line outage contingency, are shown on figures 5 - 7 respectively.

Figures 8 – 14, shows the load angle responses of generators 1, 3, 5, 7,9,11 and 13 respectively .Figures 15 - 17 shows the terminal voltage responses of generators 1, 3, and 5 respectively in that order to the transmission

Table 5: Eigenvalue and Damping Ratio of the case[9] Study Power System Buses during the Outage of the Transmission Line between Bus 31 and 29.

S/No.	Bus No.	Eigen value(λ)	Damping Ratio(ς)
1	1	0.1123±j7.0876	1.0675
2	2	0.0448±j4.0309	-0.0110
3	3	0.5526±j7.3025	0.02437
4	4	0.0547±j3.2853	0.0135
5	5	0.0413±j3.3227	-0.0124
6	6	-0.5248±j3.8483	0.1035
7	7	0.0014±j2.5144	-0.0057
8	8	0.1912±j5.808	-0.0332
9	9	0.1953±j5.716	-0.0348
10	10	0.088±j4.002	-0.022
11	11	0.4302±j3.6798	-0.4067
12	12	0.0281±j2.0154	-0.0013
13	13	-0.1212±j3.7982	-0.0324
14	14	0.0953±j3.3835	-0.0256
15	15	0.0883±j4.0012	-0.0225
16	16	0.0335±j6.852	-0.005
17	17	0.0658±j3.7896	-0.0017
18	18	0.2012±j4.3186	-0.3107
19	19	0.4029±j3.1139	-0.0108
20	20	0.0079±j2.0146	-0.2889
21	21	-0.1176±j3.1134	-0.4011
22	22	0.2021±j2.0343	-0.0003
23	23	0.3964±j4.1342	-0.2987
24	24	0.0788±j3.4342	-0.3421
25	25	0.1865±j4.0072	-0.0482

S/No.	Bus No.	Eigen value(λ)	Damping Ratio(ς)
26	26	0.2108±3.3319	-0.0569
27	27	0.0984±j2.7934	-0.1867
28	28	0.3012±j4.4310	-0.3065
29	29	0.0567±j4.0173	-0.0768
30	30	0.1684±j3.1605	-0.1347
31	31	0.2123±j5.0876	0.3675
32	32	0.0478±j3.0309	-0.2110
33	33	0.5426±j7.3025	0.02137
34	34	0.0647±j3.2253	0.0135
35	35	0.0713±j3.3427	-0.0424
36	36	-0.7248±j2.8783	0.1135
37	37	0.0014±j2.5144	-0.0057
38	38	0.1912±j5.808	-0.0332
39	39	-0.1953±j5.716	-0.0348
40	40	0.088±j4.002	-0.022
41	41	0.4302±j3.6798	-0.3107
42	42	0.0271±j2.0154	-0.0313
43	43	-0.1212±j3.7982	-0.0324
44	44	0.0753±j3.3835	-0.0256
45	45	0.0853±j4.1012	-0.0227
46	46	0.0335±j6.852	-0.0015
47	47	0.0658±j3.7896	-0.0016
48	48	0.3012±j5.3186	-0.3089

Table 6: Result of Power Flow Solution of the Case Study Power System Buses During the Outage of Transmission Line between Bus 31 and 29

Bus#	Voltage magnitude (P.u)	Voltage angle (rad)	P(P.u)	Q(P.u)
1	0.7326	-0.7817	-0.5913	-0.1086
2	0.6979	-0.5016	-0.5344	-0.1122
3	0.9328	-0.6943	-0.7676	-0.2697
4	0.4513	-0.7625	-0.5347	-0.0498
5	1.1056	-0.9227	-0.4264	-0.5617
6	0.3696	-0.3348	-0.4128	-0.9834
7	0.4934	-0.5812	-0.4576	-0.1307
8	0.7579	-0.3521	-0.5504	-0.1809
9	1.2041	-0.4817	-0.5413	-0.1086
10	0.9873	-0.4016	-0.5644	-0.1122
11	0.3934	-0.6243	-0.7646	-0.2607
12	1.0034	-0.4625	-0.5347	-0.0998
13	0.4676	-0.4227	-0.4264	-0.1017
14	0.3696	-0.3998	-0.4128	-0.1034
15	0.4986	-0.5012	-0.4576	-0.1507
16	0.7579	-0.4521	-0.5504	-0.1809
17	0.6506	-0.4332	-0.4869	-0.1264
18	0.6347	-0.3865	-0.4337	-0.1413
19	0.9717	-0.4386	-0.5812	-0.1118
20	0.9681	-0.3318	-0.5795	-0.0819
21	0.8576	-0.4626	-0.4932	-0.1338
22	0.6792	-0.3982	-0.5216	-0.2013
23	0.4647	-0.5984	-0.6937	-0.2446
24	0.3120	-0.3202	-0.4827	-0.1579
25	0.4795	-0.4529	-0.4243	-0.1834
26	1.1052	-0.4467	-0.5006	-0.1134
27	0.5613	-0.3846	-0.5138	-0.2007
28	0.8819	-0.4822	-0.5623	-0.1613

Bus#	Voltage magnitude (P.u)	Voltage angle (rad)	P(P.u)	Q(P.u)
29	0.4982	-0.4116	-0.4985	-0.1517
30	0.6813	-0.3976	-0.5963	-0.1549
31	0.9326	-0.7817	-0.5913	-0.1086
32	1.0120	-0.5016	-0.5344	-0.1122
33	0.9328	-0.6943	-0.7676	-0.2697
34	1.0123	-0.7625	-0.5347	-0.0498
35	1.0234	-0.9227	-0.4264	-0.5617
36	0.7696	-0.3348	-0.4128	-0.9834
37	0.8934	-0.5812	-0.4576	-0.1307
38	1.0325	-0.3521	-0.5504	-0.1809
39	0.5326	-0.4817	-0.5413	-0.1086
40	0.9579	-0.4016	-0.5644	-0.1122
41	0.3248	-0.6243	-0.7646	-0.2607
42	1.0045	-0.4625	-0.5347	-0.0998
43	0.8676	-0.4227	-0.4264	-0.1017
44	0.4696	-0.3998	-0.4128	-0.1034
45	0.8934	-0.5012	-0.4576	-0.1507
46	1.2067	-0.4521	-0.5504	-0.1809
47	0.9506	-0.4332	-0.4869	-0.1264
48	1.0453	-0.3865	-0.4337	-0.1413

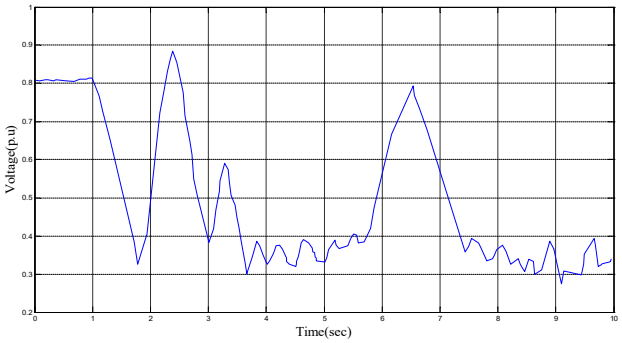

Figure5: Voltage Trajectory at Bus 11 during the Transmission Line Outage Contingency

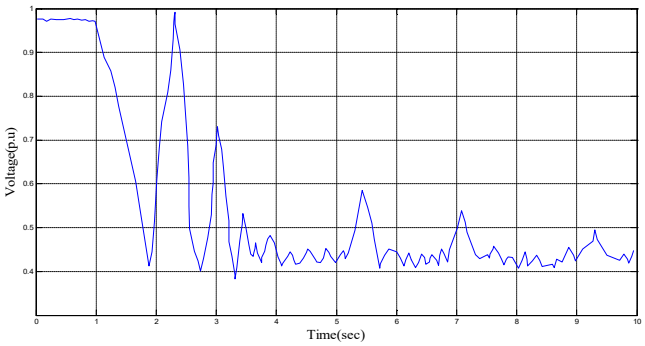

Figure 6: Voltage Trajectory at Bus 15 during the Transmission Line Outage Contingency

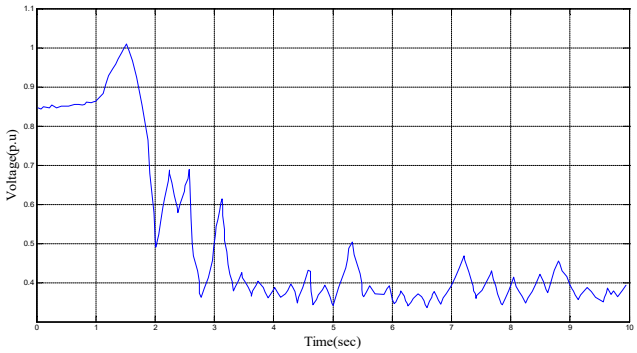

Figure 7: Voltage Trajectory at Bus 23 during the Transmission Line Outage Contingency

Figure 5 shows that at bus 11, in addition to voltage sag that began at time 1 sec, the voltage also oscillates as a result of the outage of the transmission line. It can be noticed in figure 5 – 7 that before the outage the transmission line at 1 sec, the voltages are not experiencing noticeable instabilities (i.e the voltages are fairly stable around their various operating points). Before the outage, bus 11 voltage was at 0.813 p.uoperating point, while that of 15, and 23 are around 0.987 p.u and 0.856 p.u respectively. However at the outage of transmission line at 1 sec, their voltage sagged and then oscillates.

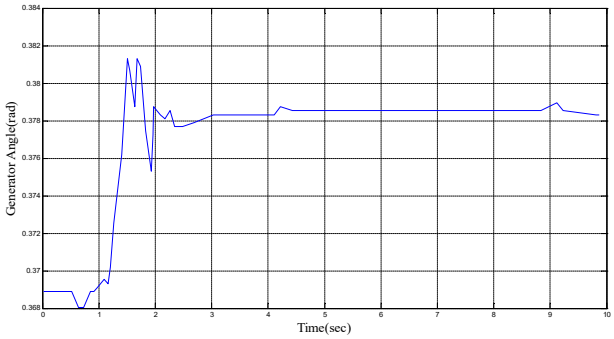

Figure 8: Generator 1 Angle Trajectory during Transmission Line Outage Contingency

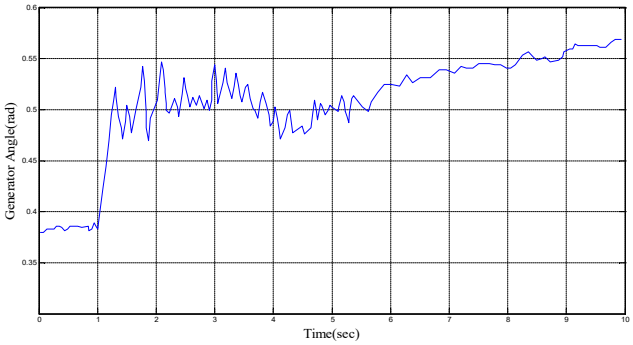

Figure 9: Generator 3 Angle Trajectory during Transmission Line Outage Contingency

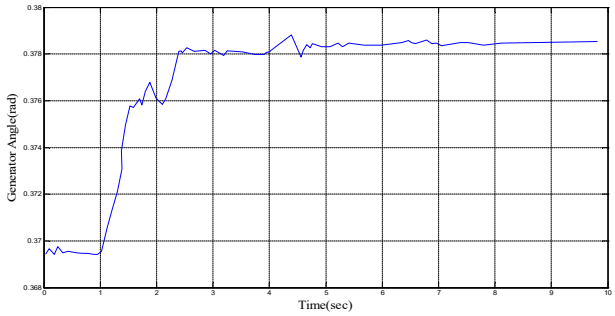

Figure10: Generator 5 Angle Trajectory during Transmission Line Outage Contingency

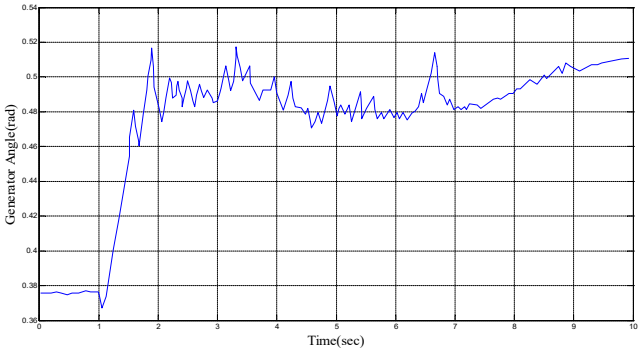

Figure11: Generator 7 Angle Trajectory during Transmission Line Outage Contingency

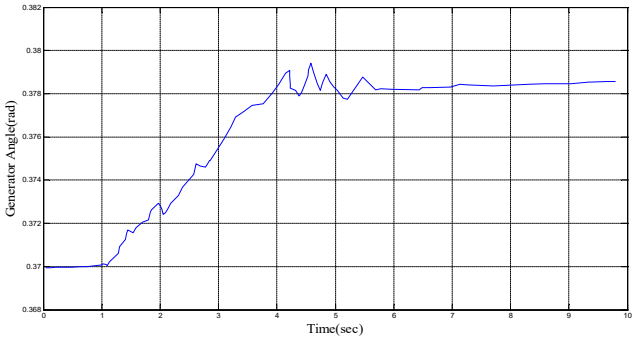

Figure 12: Generator 9 Angle Trajectory during Transmission Line Outage Contingency

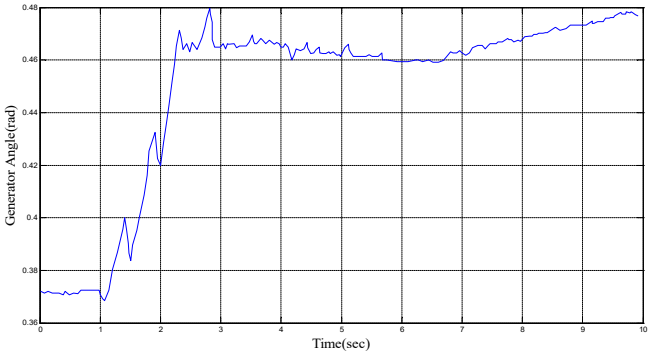

Figure 13: Generator 11 Angle Trajectory during Transmission Line Outage Contingency

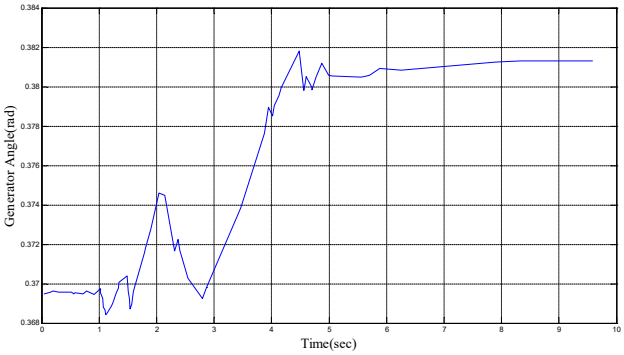

Figure 14: Generator 13 Angle Trajectory during Transmission Line Outage Contingency

From figure 8 – 14, it can be seen that at 1 sec into the simulation, from the time of transmission line outage, the angles of the generator rose then oscillates and tried to come to a new equilibrium. The larger the generator load angle, the closer it gets to the stability limit and the greater the danger of the generator falling out of

synchronism with the rest of the power system. The rise and then oscillations of the generator angle as in figure 8 – 14 indicates that the power system has become unstable.

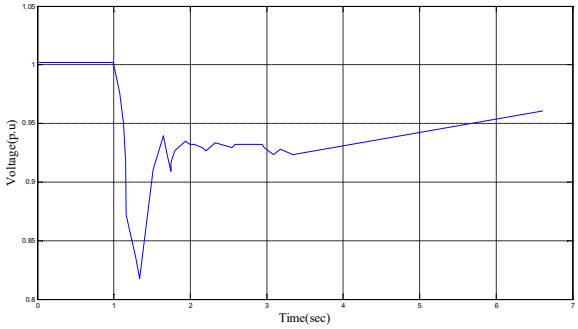

Figure 15: Generator 1 Terminal Voltage during Transmission Line Outage Contingency

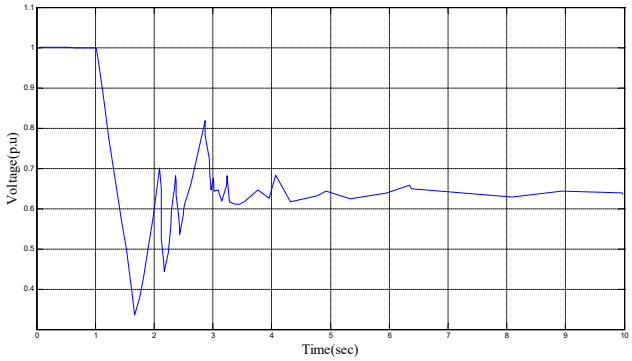

Figure 16: Generator 3 Terminal Voltage during Transmission Line Outage Contingency

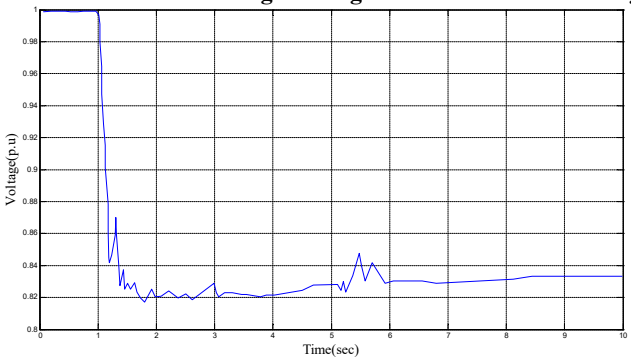

Figure 17: Generator 5 Terminal Voltage during Transmission Line Outage Contingency

The oscillation of the generator load angles is an indication of the generators' loss of synchronism with rest of the power system. The instabilities of the generators' terminal voltage as indicated in the oscillations of their terminal voltages (figure 15-17) indicates the failure of the generators excitation system and the generators AVRs to stabilize the generators output terminal voltages. These factors combine to cause the instabilities of the entire power grid as reflected in the eigenvalues and damping ratios of the buses in the power system.

The situation here requires the integration of the power system stabilizers to compliment the generator excitation system. The power system stabilizers will help to damp out the oscillations to the generator angle and the terminal voltages.

Outage of a Power Plant

The power system stability is now analyzed under generator outage condition. The MATLAB SIMULINK synchronous generator block was configured to trip the generator within a set time. The block is configured to trip generator 4 within 1.5secs of the simulation. The result of associated eigenvalue analysis is listed in table 8

Table 7: Eigen values and damping ratios of the case study power system buses for the outage of generator 4.

S/No.	Bus No.	Eigen value(λ)	Damping Ratio(ς)
1	1	0.4806±j8.1476	-0.7627
2	2	0.46302±j6.7734	-0.37414
3	3	0.4564±j5.3247	-0.3867
4	4	0.3206±j8.1476	-0.3627
5	5	0.4465±j 4.8942	-0.4019
6	6	0.4947±j 4.4366	-0.39434
7	7	0.5367±j 4.3008	-0.3762
8	8	0.4823±j5.1163	-0.4918
9	9	0.6975±j63465	-0.5328
10	10	0.6732±j 6.2248	-0.5562
11	11	0.7806±j8.1476	-0.7627
12	12	0.7453±j7.9969	-0.6834
13	13	0.7113±j6.9937	-0.7234
14	14	0.7734±j7.93644	-0.7274
15	15	0.6973±j6.9347	-0.6348
16	16	0.7389±j6.3021	-0.6849
17	17	0.7546±j7.3489	-0.6805
18	18	0.6874±j6.6534	-0.5964
19	19	0.5686±j7.7347	-0.5004
20	20	0.6896±j6.7347	-0.4908
21	21	0.7834±j8.2236	-0.6618
22	22	0.7263±j7.7993	-0.6536
23	23	0.7658±j8.8463	-0.6889
24	24	0.6835±j8.0013	-0.5876
25	25	0.5342±j6.1136	-0.4546
26	26	0.6423±j5.8376	-0.4987
27	27	0.7102±j6.3476	-0.6482
28	28	0.6659±j5.3426	-0.5586
29	29	0.7508±j6.3246	-0.6863
30	30	0.7302±j7.0034	-0.6537
31	31	0.4706±j8.1476	-0.5627
32	32	0.36302±j6.7734	-0.37414
33	33	0.4564±j5.3247	-0.3867
34	34	0.3206±j8.1476	-0.1627
35	35	0.4465±j 4.8942	-0.4019
36	36	0.6947±j 4.4366	-0.39434
37	37	0.5367±j 4.3008	-0.3762
38	38	0.4823±j5.1163	-0.6918
39	39	0.3975±j63465	-0.5328
40	40	0.6732±j 6.2248	-0.5562
41	41	0.7806±j8.1476	-0.7627
42	42	0.6353±j7.9969	-0.6834
43	43	0.6813±j6.9937	-0.7634
44	44	0.2434±j7.93644	-0.2274
45	45	0.5973±j6.9347	-0.6348
46	46	0.8389±j6.3021	-0.4849
47	47	0.2946±j7.3489	-0.9805
48	48	0.5174±j6.6534	-0.2964

From table 7, it can be seen that real part of the complex eigenvalues lie on the right-half of the S-plane. This shows that the real part of the complex eigenvalue are all positive. The damping ratios are all negative. This information indicates that the power system is unstable. Furthermore the instability from the generator outage seem to be more severe than that resulting from the transmission line outage. This is due to the fact that the real parts of the eigenvalue in table 7 of power plant outage are more positive that those of table 5 of transmission line outage, in addition the damping ratios listed in table 7 are more negative (smaller) than those listed in table 5.

Table 8 gave the output of the power flow solution carried out by ***P-flow*** using the generator outage disturbance data.

Table 8: Result of Power Flow Solution of Case Study System for the Outage of Generator 4

Bus#	Voltage magnitude (P.u)	Voltage angle (rad)	P(P.u)	Q(P.u)
1	0.5427	-0.7423	-0.8347	-0.1579
2	0.4012	-0.5276	-0.9809	-0.1834
3	0.5867	-0.9043	-0.7643	-0.1134
4	0.4216	-0.5646	-0.6217	-0.2007
5	1.002	-0.5267	-0.5784	-0.1613
6	0.7017	-0.4896	-0.5629	-0.1517
7	0.1987	-0.6876	-0.6243	-0.1549
8	0.1996	-0.6248	-0.6543	-0.1086
9	1.0231	-0.6423	-0.6347	-0.1122
10	1.0012	-0.5836	-0.9809	-0.2697
11	0.2342	-0.8643	-0.7643	-0.0498
12	0.9978	-0.5646	-0.6217	-0.5617
13	0.2213	-0.5967	-0.5784	-0.9834
14	0.3017	-0.4896	-0.5629	-0.1307
15	0.3987	-0.6876	-0.6243	-0.1809
16	0.7996	-0.6248	-0.6543	-0.1086
17	0.2003	-0.6024	-0.5567	-0.1122
18	0.6876	-0.4567	-0.5243	-0.2607
19	0.9226	-0.6132	-0.6617	-0.0998
20	0.3672	-0.4342	-0.6834	-0.1017
21	0.3214	-0.6182	-0.6324	-0.1034
22	0.7186	-0.4644	-0.6685	-0.1507
23	0.3987	-0.8835	-0.7408	-0.1809
24	0.4236	-0.4263	-0.6847	-0.1264
25	0.8106	-0.6124	-0.5246	-0.1413
26	0.3242	-0.6245	-0.6534	-0.1086
27	0.3743	-0.4168	-0.5965	-0.1122
28	0.5206	-0.6428	-0.6703	-0.2697
29	0.2459	-0.5986	-0.6136	-0.0498
30	0.3842	-0.4857	-0.6889	-0.5617
31	0.5427	-0.7423	-0.8347	-0.9834
32	0.2012	-0.5276	-0.9809	-0.1307
33	0.1867	-0.9043	-0.7643	-0.1809
34	1.0342	-0.5246	-0.6217	-0.1086
35	1.1056	-0.5267	-0.5784	-0.1122
36	0.7017	-0.4896	-0.5629	-0.2607
37	0.1987	-0.6976	-0.6243	-0.0998
38	1.1996	-0.6248	-0.6543	-0.1017
39	0.3427	-0.6123	-0.6347	-0.1034
40	0.2012	-0.5436	-0.9809	-0.1507
41	0.1867	-0.8643	-0.7643	-0.1809
42	1.0342	-0.5646	-0.6217	-0.1264
43	0.4213	-0.5967	-0.5784	-0.1413
44	0.3017	-0.4896	-0.5629	-0.1118
45	0.2987	-0.6876	-0.6243	-0.0819
46	1.1906	-0.6248	-0.6543	-0.1338
47	0.2003	-0.6024	-0.5567	-0.2013
48	0.2876	-0.4567	-0.5243	-0.2446

The voltage magnitude listed in table 8 is in line with the information from the eigenvalue and damping ratios in table 7. The voltage magnitude in table 8, indicates serious degradation in the bus voltage as a result of the power plant outage. A comparison of the levels of voltage degradation in tables 6, and table 8 showed that the severity of the voltage degradation is more than that in table 6.The severity of the degradation is worse than that of the base power system. For instance referring to the voltage levels in the result of the power flow solution in

tables 6, it can be seen that for the transmission line outage contingency, the voltage of bus 11 stood at 0.3934 p.u , that of bus 15 stood at 0.4986p.u and that of bus 23 stood at 0.4647 after the transmission line outage contingency. However for the power plant outage table 4.13, the voltage of bus 11 stood at 0.2342p.u, that of bus 15 stood at 0.3987p.u while that of bus 23 stood at 0.3987p.u. The margin gives an indication of the level of severity of the instability resulting from the outage of the power plant. This fact is shown by the very high negative damping ratio resulting from all the real parts of the bus eigenvalues lying on the right-half of the S-plane. The real parts of the eigenvalue in table 5 are very much positive than the real parts of the eigenvalues in table 7.

Figures 5 – 7 are the trajectories of the voltages at bus11, 15 and 23 respectively as the result of the outage of generator 4. The trajectories of the load angles of generator 2, 3, 5, 6, 7 and 8 as a result of the outage of generator 4 are shown by figures 21 – 23.

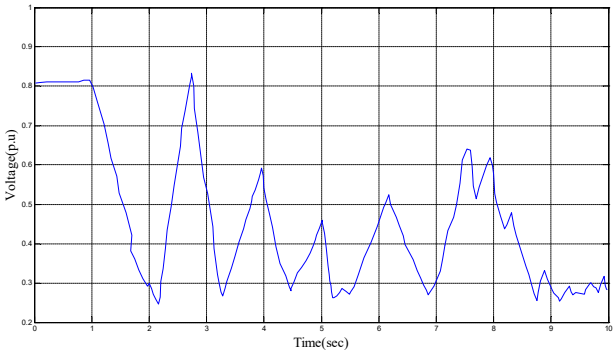

Figure 18: Voltage Trajectory at Bus 11 during the Power Plant Outage Contingency

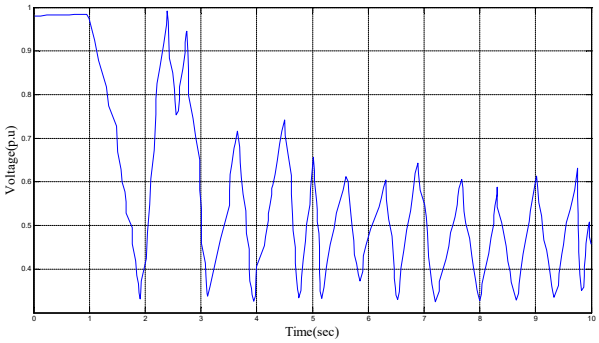

Figure 19: Voltage Trajectory at Bus 15 during the Power Plant Outage Contingency

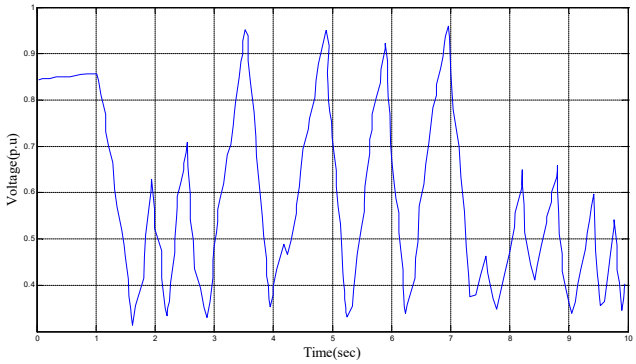

Figure 20: Voltage Trajectory at Bus 23 during the Power Plant Outage Contingency

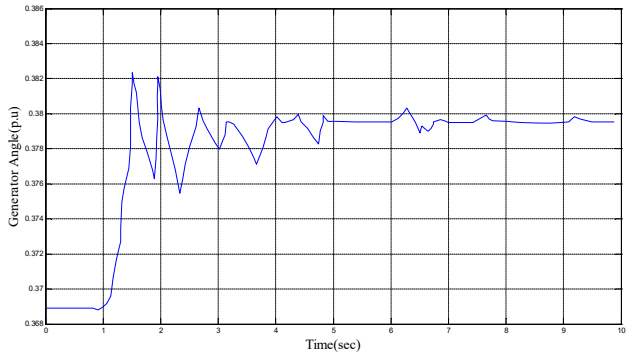

Figure 21: Generator 1 Angle Trajectory during Power Plant Outage Contingency

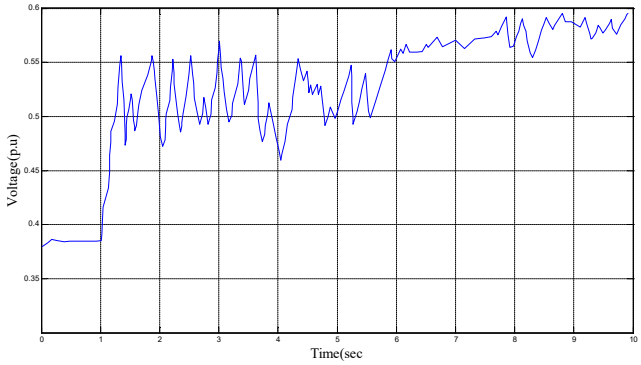

Figure 22: Generator 3 Angle Trajectory during Power Plant Outage Contingency

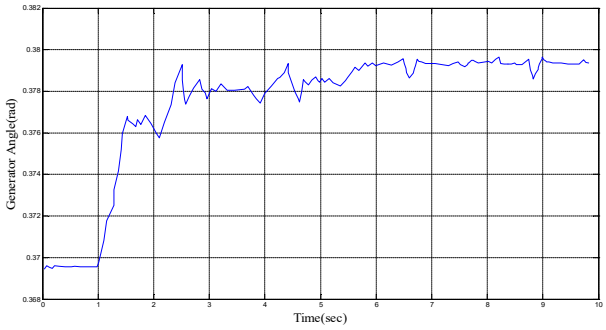

Figure 23 Generator 5 Angle Trajectory during Power Plant Outage Contingency

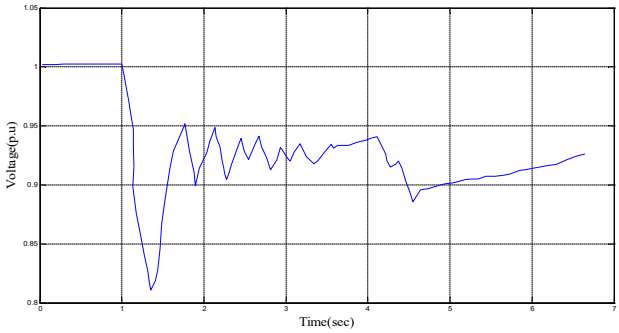

Figure 24: Generator 1 Terminal Voltage during Power Plant Outage Contingency

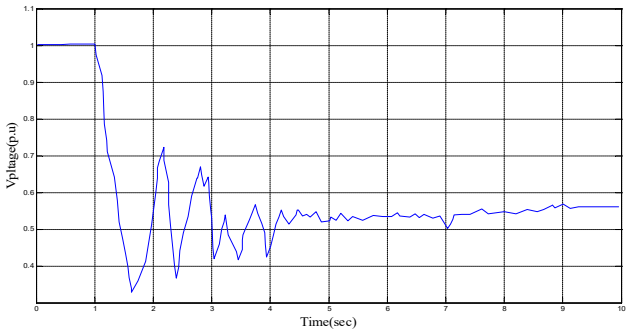

Figure 25: Generator 3 Terminal Voltage during Power Plant Outage Contingency

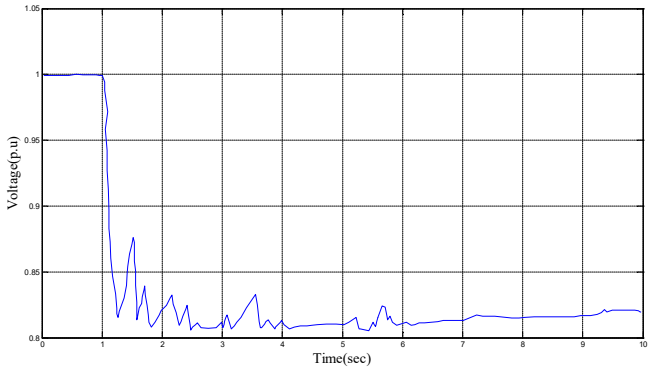

Figure 26: Generator 5 Terminal Voltage during Power Plant Outage Contingency

Figure 18 - 20 showed that the impact on the voltage levels and their stability is more severe than those of figure 5-7 in the case of the transmission line outage.

Figure 18 - 20 indicate that the voltage instability of the power system is (as seen in the level of voltage oscillations) is higher than when the power system was impacted by the transmission line outage.

The same can be said of the severity of the instability of the load angle of the generator as shown in figure 21 – 23 (for generators 1, 3, and 5), when compared to the instabilities in the case of the transmission line outage as shown in figure 8- 10. As figures 24-26 indicate the terminal voltages of the generators were heavily impacted by the power plant outage contingency more than they were impacted by the transmission line outage contingency as shown in figure 15 - 17. These results agree with the eigenvalue and damping ratio computed for the case of the transmission line outage event and the power plant outage event on the case study power plant

5.1 conclusion

It is very important to re-establish baseline values for key stability parameters for the Nigerian power system. This will enable the establishment of ground of service assessment index. From the Eigenvalue and power flow resultsof the transmission line voltage trajectories, generator terminal voltages and load angles, it is observed that the contingency impact on power plant is more severe than that of the transmission lines. This demands the need to use appropriate technique for a choice of selection of stability analysis for placement of PSS on generators with high participation factor to support the exciters of the generators. Genetic eigenvalue technique is recommended for its heuristic behavior in optimal location of eigenvalues.

References

1.Gao B., Morison G.K., &Kundar P., “Voltage Stability Evaluation using Modal Analysis”, IEEE Transaction on Power System Vol. 7, No 4,Nov.,1992.

2.Hoang P &Tomsovic K, Design and analysis of an adaptive fuzzy power system stabilizer, IEEE Transactions on Energy Conversion, 11(2), pp. 97-103,1996.

3.Kundur P. Dandeno P. L, , Lee D. C, Bayne J. P, “Impact of turbine generator controls on unit performance under system disturbance conditions,” IEEE Trans. Power Apparatus and Systems, vol. PAS-104, pp. 1262–1267, June, 2005.

4.Liu D., &Cai Y., “Taguchi method for solving the economic dispatch problem with non-smooth cost functions”, IEEE Trans. Power Syst., Vol. 20, No. 4, pp. 2006-2014, 2014

5.Lokman H. Hassan, M. Moghavvemi, Haider A.F. Almurib, K. M. Muttaqi, “A Coordinated Design of PSSs and

UPFC-based Stabilizer Using Genetic Algorithm", 10.1109/TIA .2305797, IEEE Transactions on Industry Applications, 2014.

6. Lu J, Chiang H.D, and Thorp J.S., Identification of optimum sites for power system stabilizer applications, IEEE Transactions on Power Systems, vol. 5, no. 4, pp. 1302- 1308, May, 2016.

7.Machowski J., Power System Dyromres Stability and Control, United Kingdom John Wiley and Sons, Ltd, 2008.

8.ManishaDubey. (2018), "Design of Genetic Algorithm Based Fuzzy Logic Power System Stabilizers in Multimachine Power System", 978-1-4244-1762-9/08/$25.00 © IEEE, June, 2018.10.

9.Martins N and Lima L. T. G, "Determination of suitable locations for power system stabilizers and static VAR compensators for damping electromechanical oscillations in large scale power systems," IEEE Transactions on Power Systems, vol. 5, no. 4, pp. 1455-1469. April, 2018.

10.Maslennikov V. A. and Ustinov S. M, "The optimization method for coordinated tuning of power system regulators," in Proc. 12th Power Syst. Comput. Conf. PSCC, 1996.

11.Zhou E Z., O. P. Malik, and Hope G.S., "Theory and method for selection of power system stabilizer location", IEEE Transactions on Energy Conversion, vol. 6, no. 1, pp. 170-176, 2017.

7. Mariano, S.J.P.S., Pombo, J.A.N., Calado M.R.A., Ferreira, L.A.F.M. (2010) , "Pole-shifting Procedure to specify the Weighting Matrices for an Optimal Voltage Regulator" International Review of Automatic Control (Theory and Applications), Vol. 2. n. 6, pp. 685-692.